Investigating the Domain Specificity of Phosphinic Inhibitors RXPA380 and RXP407 in Angiotensin-Converting Enzyme

ARTICLE *in* BIOCHEMISTRY · SEPTEMBER 2009

Impact Factor: 3.02 · DOI: 10.1021/bi9011226 · Source: PubMed

5 AUTHORS, INCLUDING:

Wendy Kroger
Centre for Proteomic and Genomic Research
7 PUBLICATIONS **79** CITATIONS
SEE PROFILE

Hester O'Neill
University of the Free State
23 PUBLICATIONS **367** CITATIONS
SEE PROFILE

Vincent Dive
Atomic Energy and Alternative Energies Com…
154 PUBLICATIONS **3,327** CITATIONS
SEE PROFILE

Edward D Sturrock
University of Cape Town
103 PUBLICATIONS **2,282** CITATIONS
SEE PROFILE

BIOCHEMISTRY
including biophysical chemistry & molecular biology
Article

Biochemistry **2009,** *48,* 8405–8412 8405
DOI: 10.1021/bi9011226

Investigating the Domain Specificity of Phosphinic Inhibitors RXPA380 and RXP407 in Angiotensin-Converting Enzyme[†]

Wendy L. Kröger,[‡] Ross G. Douglas,[‡] Hester G. O'Neill,[§] Vincent Dive,[∥] and Edward D. Sturrock*[,‡]

[‡]*Division of Medical Biochemistry, Institute of Infectious Disease and Molecular Medicine, University of Cape Town, Observatory, Cape Town 7935, South Africa,* [§]*Department of Biochemistry, North-West University, Potchefstroom 2531, South Africa, and* [∥]*CEA, iBiTecS, Service d'Ingénierie Moléculaire des Protéines (SIMOPRO), Gif sur Yvette F-91191, France*

Received July 2, 2009; Revised Manuscript Received August 4, 2009

ABSTRACT: Human somatic angiotensin-converting enzyme (ACE) is a membrane-bound dipeptidyl carboxypeptidase that contains two extracellular domains (N and C). Although highly homologous, they exhibit different substrate and inhibition profiles. The phosphinic inhibitors RXPA380 and RXP407 are highly selective for the C- and N-domains, respectively. A number of residues, implicated by structural data, are likely to contribute to this selectivity. However, the extent to which these different interactions are responsible for domain selectivity is unclear. In this study, a series of C- and N-domain mutants containing conversions to corresponding domain residues were used to scrutinize the contribution of these residues to selective inhibitor binding. Enzyme kinetic analyses of the purified mutants indicated that the RXPA380 C-selectivity is particularly reliant on the interaction between the P_2 substituent and Phe 391 (testis ACE numbering). Moreover, a C-domain mutant in which Phe 391 has been changed to a Tyr residue, in addition to containing an N-domain S_2' pocket (S_2'F/Y), displayed the greatest shift toward a more N-domain-like K_i. None of the single mutations within the N-domain caused a large shift in RXP407's affinity for these enzymes. However, the double mutant containing the Tyr 369 to Phe change as well as Arg 381 to Glu displayed a 100-fold decrease in binding affinity, confirming that the S_2 pocket plays a major role in RXP407 selectivity. Taken together, these data advance our understanding regarding the molecular basis for the remarkable ACE domain selectivity exhibited by these inhibitors.

Angiotensin-converting enzyme (ACE)[1], a central component of the renin−angiotensin system, is important in the regulation of blood pressure and renal and vascular function, as well as fluid and electrolyte homeostasis. The enzyme is primarily responsible for the cleavage of a dipeptide from the C-terminus of a wide range of peptide substrates, including the conversion of angiotensin I (Ang I) to the potent vasopressor angiotensin II (Ang II) and the degradation of the vasodilator bradykinin (BK). Because of this central role in blood pressure regulation, ACE is a key target for the treatment of hypertension (*1*).

ACE is a membrane-bound protein comprising intracellular, transmembrane, and glycoslated extracellular regions. Two isoforms are expressed in mammalian tissues, namely, somatic ACE (sACE) and testis ACE (tACE) (*2*, *3*). The 1227-residue ectodomain of sACE has two homologous domains, the N- and C-domains distal and proximal to the cell membrane, respectively, each containing an active site with the zinc binding motif, HEMGH. Testis ACE consists of only one extracellular domain identical to that of the C-domain of sACE and is expressed exclusively in male germinal cells (*4*).

Although the domains of sACE display 55% amino acid sequence identity, they demonstrate a number of differences, such as chloride dependence, substrate specificity, inhibition profiles (*5*, *6*), and thermostability (*7*). In terms of substrate specificity, it is known that the C-domain converts Ang I to Ang II more effectively than the N-domain, while the inactivation of BK occurs at a similar rate (*5*, *8*, *9*). While the C-domain is more prominent in Ang I conversion, natural peptides such as *N*-acetyl-Ser-Asp-Lys-Pro (AcSDKP) (*10*) and gonadotropin-releasing hormone (formally known as luteinizing hormone-releasing hormone) (*8*) have both been shown to be preferentially cleaved by the N-domain.

ACE inhibitor therapies are one of the main treatments for hypertension to date, although a number of adverse side effects have been described (*11*, *12*). These have been attributed to the excess levels of BK resulting from the complete inactivation of ACE (*13*−*15*). It has therefore been suggested that selective inhibition of the C-domain could reduce blood pressure, while allowing the N-domain to maintain normal BK levels (*1*, *16*). This would result in more effective treatment of hypertension with lowered side effects.

While the C-domain appears to have a more prominent role in blood pressure regulation, several important peptides are cleaved preferentially by the N-domain. This suggests that N-domain-selective inhibition could have beneficial consequences without alteration of blood pressure. For example, elevation of AcSDKP,

[†]This work was supported by the Wellcome Trust, U.K. (Senior International Research Fellowship 070060 to E.D.S.), the National Research Foundation, South Africa, the Stella and Paul Loewenstein Charitable and Educational Trust, the Deutscher Akademischer Austauschdienst, the Ernst and Ethel Erikson Trust, and the University of Cape Town.

*Address correspondence to this author. Telephone: +27 21 406 6312. Fax: +27 21 406 6470. E-mail: Edward.Sturrock@uct.ac.za.

[1]Abbreviations: ACE, angiotensin-converting enzyme; Ang I, angiotensin I; Ang II, angiotensin II; BK, bradykinin; sACE, somatic ACE; tACE, testis ACE; AcSDKP, *N*-acteyl-Ser-Asp-Lys-Pro; kAW, (5*S*)-5-[(*N*-benzoyl)amino]-4-oxo-6-phenylhexanoyl-L-tryptophan; kAF, (5*S*)-5-[(*N*-benzoyl)amino]-4-oxo-6-phenylhexanoyl-L-phenylalanine; CHO, Chinese hamster ovary.

Published on Web 08/06/2009

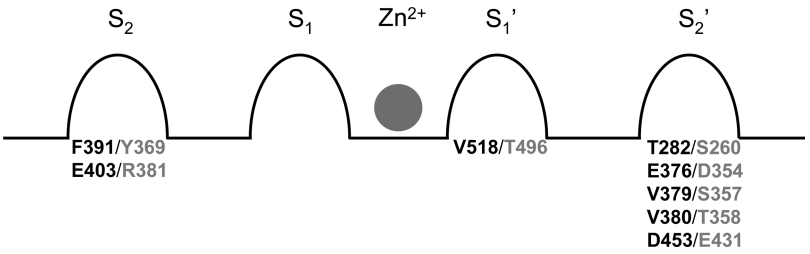

FIGURE 1: A cartoon of active site residues that differ between domains within subsite pockets (Schechter and Burger nomenclature). The catalytic zinc ion is shown as a gray circle. Subsite location of amino acid residues unique to the C-domain active site are indicated in black, while corresponding N-domain residues are in gray.

a known antifibrotic agent, via ACE N-domain inhibition could be beneficial to minimize collagen deposition in the left ventricle while maintaining normal angiotensin and blood pressure levels (*17*−*19*).

Using a number of phosphinic peptide libraries, Dive et al. were able to identify two compounds, RXP407 and RXPA380, which selectively inhibit the N- and C-domains of ACE, respectively, by approximately 3 orders of magnitude (*16*, *20*). These highly selective compounds allow for the potential development of domain-selective inhibitors with clinical relevance. It is therefore necessary to understand both the nature and extent of interactions of such inhibitors with residues in the ACE active sites.

Combinatorial synthesis of RXP407 indicated the importance of the P_2 and P_2' functional groups for N-selective binding, while a series of RXPA380 analogues implicated the S_2' pocket to play a role in the C-selectivity of this inhibitor (*20*, *21*). Furthermore, the resolution of the tACE−RXPA380 crystal structure (*22*) has revealed an important aromatic interaction between the inhibitor P_2 Phe moiety and a unique tACE S_2 residue, F391.

Structural data, while vital for rational structure-based design, do not afford the mechanistic insight mutational and enzyme kinetic data provide. Kinetic data can facilitate in determining contributions of the different active site residues toward selective inhibitor binding. For example, recently we reported structures of the C-domain cocrystallized with two C-selective keto-ACE analogues, (5*S*)-5-[(*N*-benzoyl)amino]-4-oxo-6-phenylhexanoyl-L-tryptophan (kAW) and (5*S*)-5-[(*N*-benzoyl)amino]-4-oxo-6-phenylhexanoyl-L-phenylalanine (kAF) (*23*). Kinetic analysis of domain-specific binding was assessed through the generation of C- and N-domain active site mutants and revealed several active site residues important for selective binding, thereby confirming the importance of such analysis (*23*).

The aim of this work was to understand the molecular basis of the remarkable ACE domain selectivity exhibited by RXPA380 and RXP407. Therefore, particular active site residues in both the C- and N-domains were selected (Figure 1) and mutated based on available structural and kinetic data. Their significance in the specificity of RXPA380 and RXP407, respectively, using an internally quenched, non-domain-specific fluorogenic substrate, Abz-FRK(Dnp)P-OH, was investigated. This analysis can provide valuable information for the design of novel inhibitors with clinical benefit, as well as provide a more detailed mechanistic picture of the specific binding of ACE.

EXPERIMENTAL PROCEDURES

Construction of tACE Mutants. A human tACE mutant tACEΔ36NJ (*24*), terminating at Ser 625 and lacking the region encoding the *O*-glycosylated 36 N-terminal residues, was cloned into the *Bam*HI and *Eco*RI restriction sites of pcDNA3.1(+) (Invitrogen) to facilitate expression. A series of mutants containing selected residues converted to their N-domain counterparts were generated as described previously (*23*) (Table 1, Figure 1). The same approach was used to create a number of multiple mutants by sequential site-directed mutagenesis.

Construction of N-Domain Mutants. Human soluble N-domain D629 (*25*), containing residues 1−629, was previously cloned into *Eco*RI and *Xba*I restriction sites of pcDNA 3.1(+) (Invitrogen) for expression (*26*). Introduction of mutations in the S_2 and S_2' pockets, converting residues to the corresponding C-domain residues (Figure 1), was performed using the full-length *D629* gene in pBlueScript (pBS; Strategene; Table 1). PCR-based site-directed mutagenesis was carried out using the pBS construct as described previously (*23*).

Heterologous Expression and Purification of tACE and N-Domain Mutants. All constructs, tACE and N-domain, were expressed in Chinese hamster ovary (CHO) cells (*27*). Testis ACE was purified by lisinopril affinity chromatography, as described previously (*27*, *28*). N-domain constructs were purified using the same method but required addition of NaCl to a final concentration of 800 mM in both the harvested medium and wash buffer (*29*). ACE activity was detected using a fluorogenic assay with hippurylhistidyl-leucine (Sigma) or *Z*-phenylalanyl-histidylleucine (Sigma) as a substrate (*30*, *31*). Pooled fractions were dialyzed against 2 L of 5 mM HEPES (pH 7.5) overnight. The purity of each mutant was assessed using SDS−PAGE and Coomassie staining.

Substrate Hydrolysis. Hydrolysis of the fluorogenic peptide Abz-FRK(Dnp)P-OH (a kind gift from A. Carmona, Universidade Federal de São Paulo) has been described previously (*23*, *32*). Enzyme activity was monitored in 50 mM Hepes buffer, pH 6.8, containing 200 mM NaCl and 10 μM $ZnCl_2$ by determining fluorescence at λ_{ex} = 320 nm and λ_{em} = 420 nm, at 25 °C, in triplicate using a Varian Cary Eclipse fluorescence spectrophotometer. Kinetic constants were calculated using the direct linear plot method (*33*).

Inhibition Kinetics. Stock solutions of RXPA380 and RXP407 were made by dissolving the phosphinic inhibitors in water and then diluting in 50 mM Hepes buffer, pH 6.8 (for appropriate inhibitor ionization), containing 200 mM NaCl and 10 μM $ZnCl_2$. Approximately 0.2 nM enzyme was incubated with an appropriate concentration range of inhibitor at ambient temperature for 45 min. Twenty microliters of the enzyme−inhibitor mixture was added to a substrate reaction mixture of 4 or 8 μM Abz-FRK(Dnp)P-OH in the above-mentioned buffer to make up a total volume of 300 μL. Residual enzyme activity was monitored by determining fluorescence using the approach described in substrate hydrolysis. Inhibition constants were calculated using the Dixon method (*34*).

Table 1: Summary of tACE and N-Domain Mutants and Their Kinetic Parameters (K_m and k_{cat}) for Abz-FRK(Dnp)P-OH Hydrolysis[a]

mutant	pocket	tACE residues	N-domain residue	K_m (μM)	k_{cat} (s^{-1})
tACE (C-domain)				3.9	25.6
T282S[b]	S_2'	Thr 282	Ser 260	5.0	1.2
E376D[b]	S_2'	Glu 376	Asp 354	9.9	0.6
V379S[b]	S_2'	Val 379	Ser 357	5.9	29.6
V380T[b]	S_2'	Val 380	Thr 358	10.6	27.0
VV379,380ST[b]	S_2'	Val 379, Val 380	Ser 357, Thr 358	6.8	33.0
D453E[b]	S_2'	Asp 453	Glu 431	5.5	5.5
V518T[b]	S_1	Val 518	Thr 496	12.0	6.9
F391Y[b]	S_2	Phe 391	Tyr 369	10.3	4.5
E403R[b]	S_2	Glu 403	Arg 381	3.7	30.2
TEVD[b]	S_2'	Thr 282, Glu 376, Val 380, Asp 453	Ser 260, Asp 354, Thr 358, Glu 431	26.8	27.7
TEVVD[b]	S_2'	S_2' pocket	Ser 260, Asp 354, Ser 357, Thr 358, Glu 431	18.4	36.8
S_2'F/Y[b]	S_2', S_2	S_2', F391	combined S_2' and Tyr 369	6.7	28.8
N-domain				3.7	11.4
Ndom S357V[c]	S_2'	Val 379	Ser 357	7.0	2.6
Ndom T358V[c]	S_2'	Val 380	Thr 358	4.9	5.1
Ndom Y369F[c]	S_2	Phe 391	Tyr 369	12.6	3.9
Ndom R381E[c]	S_2	Glu 403	Arg 381	11.7	10.8
Ndom ST357,358VV[c]	S_2'	Val 379, Val 380	Ser 357, Thr 358	5.0	0.26
Ndom YR369,381FE[c]	S_2	Phe 391, Glu 403	Tyr 369, Arg 381	8.14	25.0

[a]Cleavage of the fluorogenic peptide substrate Abz-FRK(Dnp)P-OH by a series of tACE and N-domain active site mutants was analyzed. Initial velocities for at least seven substrate concentrations were determined in triplicate, and kinetic constants were calculated using the direct linear plot method (*33*). [b]tACE (C-domain) construct containing mutation(s) converting the indicated C-domain residue to the corresponding N-domain residue. [c]N-domain construct containing mutation(s) converting the indicated N-domain residue to the corresponding tACE residue.

RESULTS

Despite high sequence similarity between the domains of sACE, differences in inhibitor selectivities are observed, suggesting that changes in amino acid composition within the active sites play a role in inhibitor selectivity. Previously, several unique active site residues in the C- and N-domains of ACE were indicated to interact with the two phosphinic inhibitors using a cocrystal structure of RXPA380 and tACE (*22*) as well as several docked structures of RXP407 with the N-domain (*26*, *35*, *36*). Therefore, unique residues in the obligatory binding site of each domain (N and C) were converted to their corresponding domain counterparts in order to assess the effects of such conversions on the selectivity of phosphinic inhibitors, RXPA380 and RXP407 (Table 1). These mutants were expressed in CHO cells and purified via lisinopril affinity chromatography.

Hydrolysis of Abz-FRK(Dnp)P-OH. To analyze the catalytic integrity of each construct, kinetic constants were calculated for each mutant using the fluorogenic peptide Abz-FRK(Dnp)P-OH. Under the conditions described in the Experimental Procedures, Abz-FRK(Dnp)P-OH demonstrated a similar affinity for both the C- and N-domains, with K_m values of 3.9 and 3.7 μM, respectively (Table 1), consistent with previously published data (*32*). All mutants displayed K_m values similar to those of the wild-type enzymes; however, there was greater variation among the k_{cat} values. For example, the TEVVD mutant displayed the highest value of 37 s^{-1} while the lowest value of 0.26 s^{-1} was obtained for Ndom ST357,358VV (Table 1).

Domain Selectivity of RXPA380. RXPA380 demonstrated C-domain-specific inhibition of the hydrolysis of the fluorogenic peptide Abz-FRK(Dnp)P-OH, with an 880-fold higher affinity for the C-domain than for the N-domain (Table 2). This inhibitor was then analyzed for its selectivity toward a series of tACE mutants containing corresponding N-domain active site substitutions.

Of the single residue S_2' pocket mutants, V380T demonstrated the highest increase in K_i, approximately 7-fold over that of tACE (Table 2, Figure 2). The V379S mutation caused a 2-fold decrease in K_i compared to the C-domain (Table 2, Figure 2). The corresponding N-domain mutant, Ndom S357V (Table 1), containing the tACE Val in this position demonstrated a further decrease in affinity for RXPA380 compared to that of the N-domain (Table 2). The double mutant VV379,380ST and single mutants E376D, D453E, and T282S demonstrated only modest increases in K_i values of 2.6-, 5.3-, 4.2-, and 3.6-fold, respectively (Table 2, Figure 2).

Table 2: Kinetic Parameters for the Inhibition of ACE by RXPA380 and RXP407[a]

mutants	pocket	RXP407 K_i (nM)	RXPA380 K_i (nM)
tACE		2800	69.0
T282S	S_2'	nd[b]	251
E376D	S_2'	nd[b]	363
V379S	S_2'	330	36.4
V380T	S_2'	800	462
VV379,380ST	S_2'	1100	177
D453E	S_2'	nd[b]	288
V518T	S_1	11000	276
F391Y	S_2	1500	2326
E403R	S_2	1800	97.5
TEVD	S_2'	6600	2236
TEVVD	S_2'	760	1160
S_2'F/Y	S_2'/S_2	16.1	5300
N-domain		5.2	60900
Ndom S357V	S_2'	20.5	320000
Ndom T358V	S_2'	3.4	nd[b]
Ndom Y369F	S_2	18.0	21600
Ndom R381E	S_2	33.5	nd[b]
Ndom ST357,358VV	S_2'	3.6	nd[b]
Ndom YR369,381FE	S_2	631	nd[b]

[a]Inhibition constants for wild-type tACE and the N-domain, as well as active site mutants containing corresponding N- and C-domain active site residue substitutions, using the fluorogenic peptide substrate Abz-FRK-(Dnp)P-OH, were determined using the Dixon method (*34*). Initial velocities for at least seven inihibitor concentrations were determined in triplcate, at different substrate concentrations. [b]Not determined.

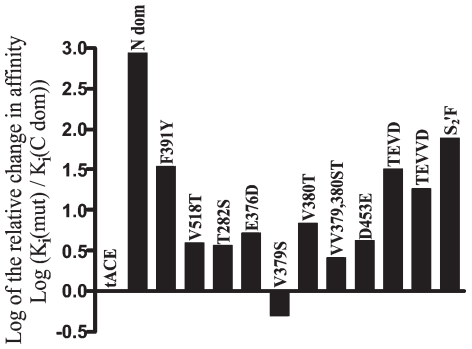

FIGURE 2: Logarithmic scale comparison of the relative binding affinity of tACE active site mutants for RXPA380 with that of wild-type tACE (C-domain). Values above zero represent a decrease in affinity relative to that of tACE, toward a more N-domain-like K_i.

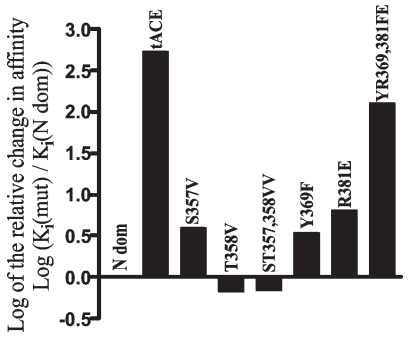

FIGURE 3: Logarithmic scale comparison of the relative binding affinity of N-domain active site mutants for RXP407 with that of the wild-type N-domain. Values above zero represent a decrease in affinity relative to the unmutated N-domain toward a more C-domain-like K_i.

In assessing multiple S_2' mutants, the TEVD mutant displayed a 32-fold increase in K_i in relation to tACE, compared to the 16-fold increase observed with the quintuple TEVVD pocket mutant (Table 2, Figure 2).

The effect of the S_1 V518 replaced with a Thr residue was investigated and shown to cause a 4-fold increase in K_i from that of the wild-type tACE (Table 2, Figure 2). This shift is probably a result of the decrease in hydrophobicity resulting from the Val to Thr substitution and is consistent with previous data reported for the keto-ACE derivatives (*23*). Analysis of the S_2 F391Y mutant, however, revealed the highest shift in K_i for RXPA380 observed for all of the single mutations, a 34-fold decrease in affinity relative to tACE (Table 2, Figure 2), while the corresponding N-domain mutant, Ndom Y369F (Table 1), displayed a reciprocal, albeit less marked, increase in RXPA380 binding affinity compared to the wild-type N-domain (Table 2).

The tACE construct S_2'F/Y, containing an N-domain S_2' pocket as well as the S_2 F391Y mutation, was used to investigate the combined contribution of these subsites to domain selectivity. This mutant displayed an approximately 80-fold increase in K_i compared to the C-domain, the highest increase observed among all of the tACE mutations (Table 2, Figure 2).

Domain Selectivity of RXP407. In contrast to RXPA380, RXP407 demonstrated an approximately 550-fold selectivity for the N-domain (N-domain K_i = 5.16 nM; C-domain K_i = 2.8 μM; Table 2).

In order to investigate the effect of particular residues on RXP407 binding, we mutated unique active site residues within the N-domain to their corresponding tACE counterparts (Table 1). Surprisingly, however, single mutations in both the S_2 and S_2' pockets resulted in only modest increases in K_i from that of the wild-type N-domain (Table 2). Introduction of two S_2' mutations (Ndom ST357,358VV, Table 1) did not notably decrease the affinity of RXP407 for the double mutant active site. Interestingly, however, the S_2 double mutant, Ndom YR369,381FE (Table 1), rendered an increase in K_i more than 100-fold compared to that of the wild-type N-domain (Table 2, Figure 3).

To further explore the molecular basis of RXP407 domain selectivity, the single and multiple tACE mutants described above (Table 1) were tested to analyze the effect of mutations on the affinity of the inhibitor. As with the N-domain single mutations, individual substitutions within these pockets had little effect on their affinity for this inhibitor (Table 2). Interestingly, while the tACE construct containing an N-domain-like S_2' pocket (TEVVD, Table 1) caused a slight decrease in K_i, approximately 4-fold from that of tACE (Table 2), this construct combined with the F391Y mutation (S_2'F/Y) resulted in a shift in affinity of approximately 175-fold, demonstrating a K_i only 3-fold higher than that of the N-domain.

DISCUSSION

Despite sequence similarity between the N- and C-domains, the phosphinic inhibitors RXPA380 and RXP407 display marked ACE C- and N-selectivity. The relative contributions of key active site residues unique to each domain toward such selectivities will provide (1) an understanding of mechanism(s) of inhibitor binding action and (2) useful insight into the design of domain-specific ACE inhibitors with possible therapeutic benefit.

Initial kinetic assessment analyzed the catalytic activity of the mutants. Variations among k_{cat} values are usually a result of effects on the formation of the tetrahedral intermediate. However, the RXPA380−tACE crystal structure revealed that, of the substitutions tested, only V518 is within 7 Å of the residues stabilizing the transition state (K511, H513, and Y520) (*22*). These substitutions are therefore unlikely to have a direct effect on hindering the formation of this intermediate and may be possible that these conversions cause a change in the orientation of the substrate molecule, which might result in unfavorable or more efficient interaction with these stabilizing residues, thereby reducing the efficacy with which the substrate is cleaved. The lowered catalytic efficiency observed for V518T could be attributed to a change in conformation of the transitions state H513, as a result of favorable interactions introduced with the replacement of this Val moiety with the corresponding N-domain Thr.

RXPA380 demonstrated a marked C-domain selectivity (Table 2). Surprisingly, single N-domain substitutions within the S_2' and S_1 pockets had minor effects on this selectivity. The decrease in affinity observed for V380T is probably due to a reduction in hydrophobicity within the S_2' subsite, caused by the Val to Thr substitution (Figure 4), which is in agreement with suggestions by a previous study (*21*). In that study, the P_2' pseudo-Trp moiety was identified as potentially conferring the selectivity observed with this inhibitor, particularly the hydrophobic interactions of this group with the C-domain V379 and V380 residues. These interactions would be lost in the N-domain (replaced with S357 and T358).

Interestingly, however, the V379S mutation caused an opposite effect on binding of RXPA380 to what was expected (Table 2, Figure 2). This phenomenon has been previously observed with the C-domain-selective inhibitor kAW, which

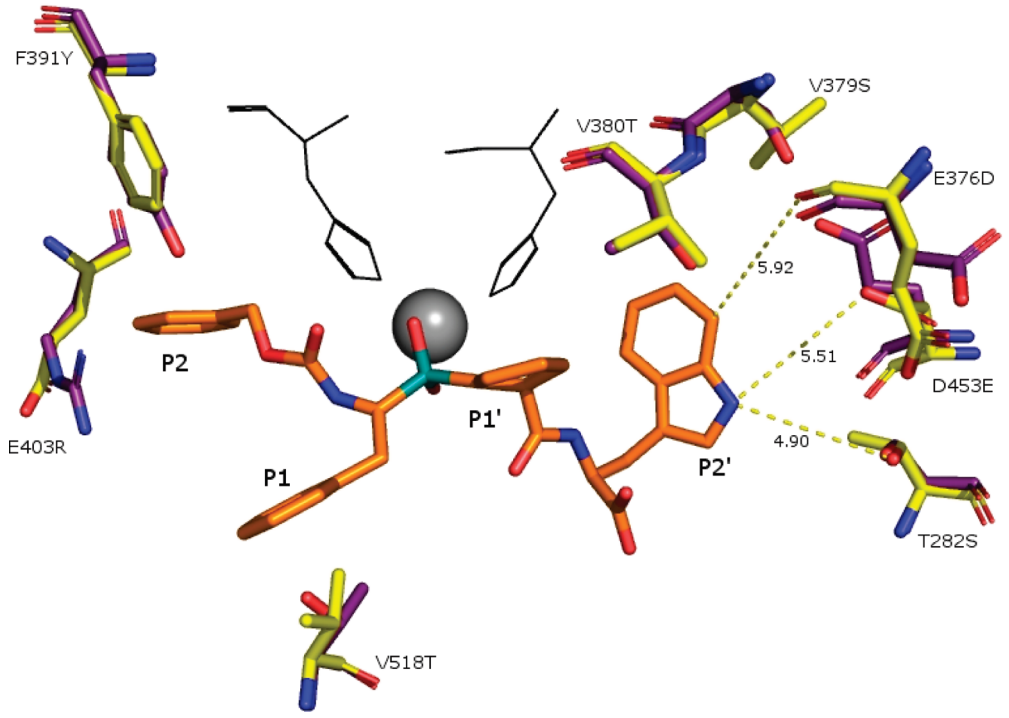

FIGURE 4: Stick representation of RXPA380 (orange) within the active site of tACE (PDB code 2OC2) aligned to the N-domain (PDB code 2C6F). Residues differing between tACE and the N-domain are shown in yellow and purple sticks, respectively. The position of the active site zinc ion is indicated as a gray sphere, two of the zinc-chelating residues (His 383 and His 387) are shown as black lines, and the inhibitor's carbon and phosphorus atoms are in orange and cyan, respectively. All distances are given in angstroms (Å). Alignments were performed using the program ALIGN (*37*) and images manipulated with PyMOL software (DeLano Scientific, LLC).

also has a Trp in the P_2' position (*23*). Although an explanation for this result is not clear from the RXPA380−tACE crystal structure, it has been suggested to be a consequence of hydrogen bond formation between the mutant Ser and the indole N of the inhibitor Trp via a water molecule (*23*). This process may be facilitated by rearrangement of S_2' pocket residues and the inhibitor side chains (Figure 4). This was supported by the absence of any change in affinity observed for the V379S mutant with the C-domain-selective inhibitor kAF, containing a Phe in this position and therefore lacking a hydrogen bond acceptor (*23*). This idea is further emphasized by the decrease in RXPA380 affinity observed for the Ndom S357V mutant (Table 2). This construct contains a Val in this position and therefore lacks a hydrogen bond donor group.

Only minimal changes in K_i were observed for S_2' mutants E376D and D453E (Table 2, Figure 2). The distances of residues E376 and D453 from the inhibitor Trp are 5.92 and 5.51 Å, respectively (Figure 4), as seen in the RXPA380−tACE cocrystal structure. Hence, due to the space available within this subsite, the design of compounds with more extensive substituents at the P_2' position could potentially lead to considerably increased domain-specific inhibition.

To further understand the results obtained with the single S_2' mutants and investigate synergistic effects of the interactions, two multiple tACE mutants were generated: one containing an N-domain S_2' pocket (TEVVD), where all of the unique C-domain residues were substituted with their N-domain counterparts, and a similar construct lacking the V379S mutation (TEVD) (Table 1). The combined effect of the unique TEVD mutant suggests that there is an additive effect within this pocket (Figures 2 and 4). Furthermore, the presence of a Val at position 379 in tACE (or position 357 in the N-domain) seems to decrease affinity for RXPA380, while the presence of a Ser in this position causes the opposite effect. These data emphasize the limitations of a static model derived from the X-ray data of an enzyme−inhibitor complex and the importance of kinetic and biochemical analyses that take into account the dynamics of the protein's active site and its ligand.

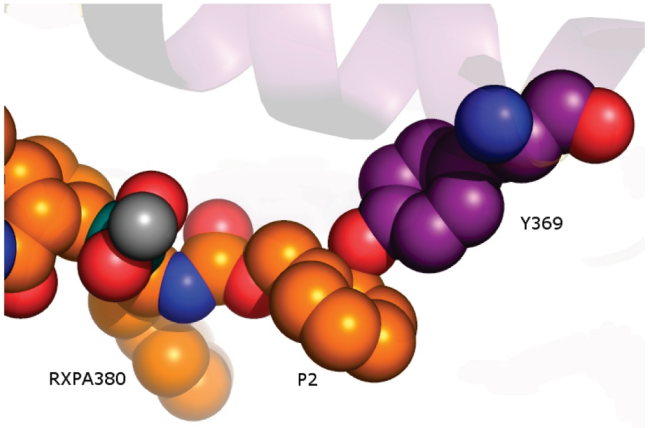

FIGURE 5: Sphere representation of RXPA380 (orange) and the N-domain Y369 (tACE F391) in purple. The N-domain structure (2C6F) was aligned to the tACE−RXPA380 cocrystal structure (2OC2). It is clear that there may be steric clash within this pocket (S_2), resulting in the inhibitor adopting a different orientation. Alignments were performed using the program ALIGN (*37*) and images manipulated with PyMOL software (DeLano Scientific, LLC).

Of all of the single mutations, the S_2 pocket F391Y caused the biggest increase in K_i (Table 2, Figure 2). The tACE−RXPA380 crystal structure (PDB code 2OC2) revealed an aromatic interaction between the N-terminal pseudo-Phe side chain of the inhibitor and F391 of tACE in the S_2 pocket (*22*). This interaction seems to be responsible for the positioning of RXPA380 within

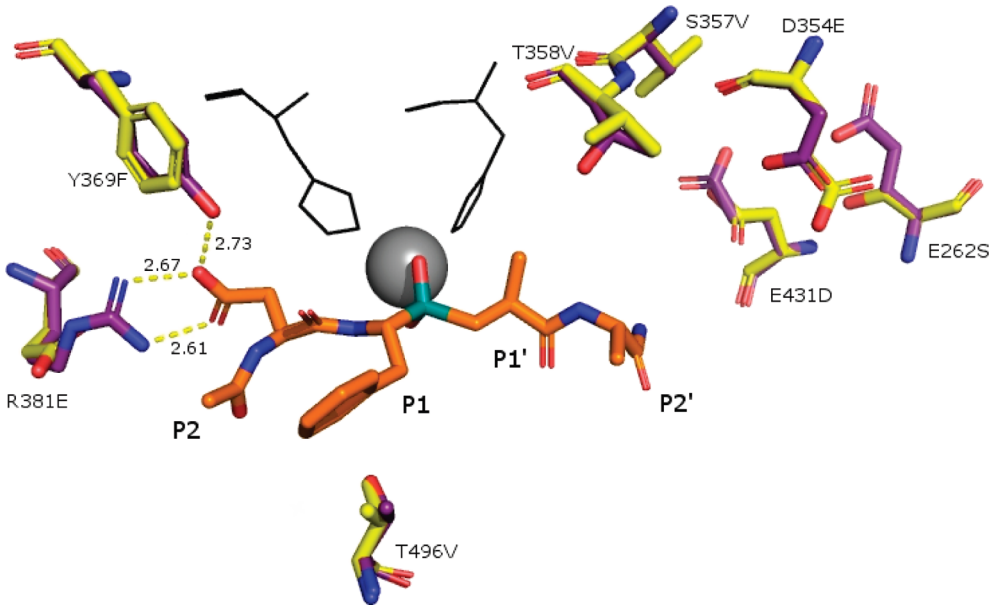

FIGURE 6: Stick representations of RXP407 (orange) within the active site of the homology-modeled N-domain as performed by Jullien et al. (*35*). The modeled complex was aligned to the tACE−lisinopril cocrystal structure (PDB code 1O86). Residues differing between tACE and the N-domain are shown in yellow and purple sticks, respectively. The position of the active site zinc ion is indicated as a gray sphere, two of the zinc-chelating residues (His 383 and His 387) are shown as black lines, and the inhibitor's carbon and phosphorus atoms are in orange and cyan, respectively. All distances are given in angstroms (Å). Alignments were performed using the program ALIGN (*37*) and images manipulated with PyMOL software (DeLano Scientific, LLC).

the active site and would be lost in the N-domain, where the Phe residue is replaced by Y369 (Figure 4). Furthermore, the Tyr hydroxyl might result in a steric clash with the P_2 Phe of RXPA380 (Figure 5) which could result in a different orientation of the inhibitor in the N-domain. Therefore, based on the X-ray structure and mutational kinetic analysis, it is likely that F391 makes an important contribution to the C-domain specificity of this inhibitor.

The most N-domain-like RXPA380-binding character was observed by a mutant combining substitutions within the S_2' and S_2 pockets, S_2'F/Y (Table 2, Figure 2). Although there was an 80-fold decrease in affinity for RXPA380 compared to that of the C-domain, this inhibitor still demonstrated an approximately 10-fold higher affinity for this construct than for the wild-type N-domain, suggesting that there must be additional factors contributing to the marked selectivity of this inhibitor, such as scaffolding residues stabilizing the conformation or positioning of conserved residues important for selective binding.

In contrast to RXPA380, RXP407 displayed a 550-fold higher affinity for the N-domain (Table 2), results comparable with previous findings (*16*, *20*, *21*). Single substitutions in the N-domain active site did not result in large reductions in RXP407 binding affinity (Figure 3). With the seemingly limited role observed for individual residues in conferring N-selectivity, we investigated the effect of double mutants of the above residues.

Interestingly, two S_2' conversions in the N-domain (Ndom ST357,358VV, Table 1) had a similar affinity for RXP407 compared to that of the wild type (Table 2, Figure 3), while a double mutation within the S_2 pocket (Ndom YR369,381FE, Table 1) caused a greater than 100-fold increase in K_i for this inhibitor (Table 2, Figure 3). These data, along with the individual mutations having modest effects on K_i values, suggest that the presence of either Y369 or R381 is sufficient to position RXP407 and allow prominent N-selective binding.

The concept of the S_2 pocket playing the major role in selectivity is consistent with the original report of RXP407 synthesis (*20*), where it was shown that the presence of an aspartate residue and *N*-acetyl group in the P_2 position was important for the selectivity of RXP407. Moreover, while the P_2' alanine was less important, as no residues in this position conferred major N-selective inhibition, the presence of an amidated C-terminus contributes to the selectivity of this compound. Further investigation is required to understand the contribution of the protecting group and S_2' residues in N-selectivity.

No RXP407−N-domain crystal structure is presently available. However, several docked structures have been modeled, with differences in inhibitor orientation and hence residue contacts. Utilizing the N-domain crystal structure, Corradi et al. proposed Y369 alone interacts with the *N*-acetyl group of RXP407 (*26*). Jullien et al. (*35*) as well as Tzakos and Gerothanassis (*36*) made use of homology modeling and suggested that Y369 and R381 both interact closely with the inhibitor. Based on the previously reported importance of the P_2 aspartate and *N*-acetyl group of RXP407 in N-selectivity (*20*), as well as the data presented here, it seems the models whereby the P_2 group interacts with both Y369 and R381 are more compelling (Figure 6). However, the model proposed by Corradi et al. could still be relevant in describing an orientation where R381 is mutated and RXP407 can still bind to this mutant active site with relatively high affinity. Further kinetic studies of other active site mutants and crystal structure determination are required in order to refine and confirm the current models.

Testing the affinity of RXP407 for tACE mutants rendered similar results to the N-domain mutants for the discrete substitutions, where only slight changes in affinity were observed (Table 2). Interestingly, the full S_2' pocket substitutions combined with the S_2 F391Y conversion yielded a protein with a K_i 175-fold lower than that of wild-type tACE, while this construct lacking the S_2 mutation displayed only a 4-fold decrease (Table 2). This highlights the fact that ACE domain selectivity is the result of a combination of residues in different active site pockets.

We have shown that a number of residues within the active site of tACE play a significant role in the domain selectivity of RXPA380. In particular, F391 as well as a number of residues within the S_2' pocket, as demonstrated by the S2′F/Y construct, seem to have an additive effect in the marked C-domain selectivity of this inhibitor. In terms of N-selectivity, the presence of either Y369 or R381 allows for RXP407 to bind selectively to the N-domain active site, with the S_2' residues studied playing no prominent roles in this selectivity. Based on this work, it can be suggested that the incorporation of a moiety that interacts favorably with the F391 residue, while utilizing the S_2' pocket more extensively, could lead to other C-domain-specific inhibitors. Furthermore, design of N-selective inhibitors should optimize the interactions with Y369 and R381. In addition, we have shown the importance of kinetic data in understanding the mechanistic basis of the N- and C-domain active sites and the role such a mechanism plays in specific binding of inhibitors.

This work paves the way for a more rational design of domain-selective ACE inhibitors based on both the structural and functional aspects of ACE. Such inhibitors could be of clinical benefit including, but not limited to, cardiovascular disease states.

ACKNOWLEDGMENT

We thank Dr. Jean Watermeyer for helpful comments on the manuscript, as well as Dr. Geofrey Arinaitwe (Kawanda Agricultural Research Institute, Uganda) for technical assistance.

REFERENCES

1. Acharya, K. R., Sturrock, E. D., Riordan, J. F., and Ehlers, M. R. (2003) Ace revisited: a new target for structure-based drug design. *Nat. Rev. Drug Discov. 2*, 891–902.
2. Soubrier, F., Alhenc-Gelas, F., Hubert, C., Allegrini, J., John, M., Tregear, G., and Corvol, P. (1988) Two putative active centers in human angiotensin I-converting enzyme revealed by molecular cloning. *Proc. Natl. Acad. Sci. U.S.A. 85*, 9386–9390.
3. Ehlers, M. R., Fox, E. A., Strydom, D. J., and Riordan, J. F. (1989) Molecular cloning of human testicular angiotensin-converting enzyme: the testis isozyme is identical to the C-terminal half of endothelial angiotensin-converting enzyme. *Proc. Natl. Acad. Sci. U.S.A. 86*, 7741–7745.
4. Langford, K. G., Zhou, Y., Russell, L. D., Wilcox, J. N., and Bernstein, K. E. (1993) Regulated expression of testis angiotensin-converting enzyme during spermatogenesis in mice. *Biol. Reprod. 48*, 1210–1218.
5. Wei, L., Alhenc-Gelas, F., Corvol, P., and Clauser, E. (1991) The two homologous domains of human angiotensin I-converting enzyme are both catalytically active. *J. Biol. Chem. 266*, 9002–9008.
6. Wei, L., Clauser, E., Alhenc-Gelas, F., and Corvol, P. (1992) The two homologous domains of human angiotensin I-converting enzyme interact differently with competitive inhibitors. *J. Biol. Chem. 267*, 13398–13405.
7. Voronov, S., Zueva, N., Orlov, V., Arutyunyan, A., and Kost, O. (2002) Temperature-induced selective death of the C-domain within angiotensin-converting enzyme molecule. *FEBS Lett. 522*, 77–82.
8. Jaspard, E., Wei, L., and Alhenc-Gelas, F. (1993) Differences in the properties and enzymatic specificities of the two active sites of angiotensin I-converting enzyme (kininase II). Studies with bradykinin and other natural peptides. *J. Biol. Chem. 268*, 9496–9503.
9. Fuchs, S., Xiao, H. D., Hubert, C., Michaud, A., Campbell, D. J., Adams, J. W., Capecchi, M. R., Corvol, P., and Bernstein, K. E. (2008) Angiotensin-converting enzyme C-terminal catalytic domain is the main site of angiotensin I cleavage in vivo. *Hypertension 51*, 267–274.
10. Rousseau, A., Michaud, A., Chauvet, M. T., Lenfant, M., and Corvol, P. (1995) The hemoregulatory peptide N-acetyl-Ser-Asp-Lys-Pro is a natural and specific substrate of the N-terminal active site of human angiotensin-converting enzyme. *J. Biol. Chem. 270*, 3656–3661.
11. Bicket, D. P. (2002) Using ACE inhibitors appropriately. *Am. Fam. Physician 66*, 461–468.
12. Morimoto, T., Gandhi, T. K., Fiskio, J. M., Seger, A. C., So, J. W., Cook, E. F., Fukui, T., and Bates, D. W. (2004) An evaluation of risk factors for adverse drug events associated with angiotensin-converting enzyme inhibitors. *J. Eval. Clin. Pract. 10*, 499–509.
13. Nussberger, J., Cugno, M., Amstutz, C., Cicardi, M., Pellacani, A., and Agostoni, A. (1998) Plasma bradykinin in angio-oedema. *Lancet 351*, 1693–1697.
14. Beltrami, L., Zingale, L. C., Carugo, S., and Cicardi, M. (2006) Angiotensin-converting enzyme inhibitor-related angioedema: how to deal with it. *Expert Opin. Drug Saf. 5*, 643–649.
15. Ehlers, M. R. (2006) Safety issues associated with the use of angiotensin-converting enzyme inhibitors. *Expert Opin. Drug Saf. 5*, 739–740.
16. Georgiadis, D., Beau, F., Czarny, B., Cotton, J., Yiotakis, A., and Dive, V. (2003) Roles of the two active sites of somatic angiotensin-converting enzyme in the cleavage of angiotensin I and bradykinin: insights from selective inhibitors. *Circ. Res. 93*, 148–154.
17. Peng, H., Carretero, O. A., Raij, L., Yang, F., Kapke, A., and Rhaleb, N. E. (2001) Antifibrotic effects of N-acetyl-seryl-aspartyl-lysyl-proline on the heart and kidney in aldosterone-salt hypertensive rats. *Hypertension 37*, 794–800.
18. Peng, H., Carretero, O. A., Liao, T. D., Peterson, E. L., and Rhaleb, N. E. (2007) Role of N-acetyl-seryl-aspartyl-lysyl-proline in the antifibrotic and anti-inflammatory effects of the angiotensin-converting enzyme inhibitor captopril in hypertension. *Hypertension 49*, 695–703.
19. Cavasin, M. A., Liao, T. D., Yang, X. P., Yang, J. J., and Carretero, O. A. (2007) Decreased endogenous levels of Ac-SDKP promote organ fibrosis. *Hypertension 50*, 130–136.
20. Dive, V., Cotton, J., Yiotakis, A., Michaud, A., Vassiliou, S., Jiracek, J., Vazeux, G., Chauvet, M. T., Cuniasse, P., and Corvol, P. (1999) RXP 407, a phosphinic peptide, is a potent inhibitor of angiotensin I converting enzyme able to differentiate between its two active sites. *Proc. Natl. Acad. Sci. U.S.A. 96*, 4330–4335.
21. Georgiadis, D., Cuniasse, P., Cotton, J., Yiotakis, A., and Dive, V. (2004) Structural determinants of RXPA380, a potent and highly selective inhibitor of the angiotensin-converting enzyme C-domain. *Biochemistry 43*, 8048–8054.
22. Corradi, H. R., Chitapi, I., Sewell, B. T., Georgiadis, D., Dive, V., Sturrock, E. D., and Acharya, K. R. (2007) The structure of testis angiotensin-converting enzyme in complex with the C domain-specific inhibitor RXPA380. *Biochemistry 46*, 5473–5478.
23. Watermeyer, J. M., Kröger, W. L., O'Neill, H. G., Sewell, B. T., and Sturrock, E. D. (2008) Probing the basis of domain-dependent inhibition using novel ketone inhibitors of angiotensin-converting enzyme. *Biochemistry 47*, 5942–5950.
24. Yu, X. C., Sturrock, E. D., Wu, Z., Biemann, K., Ehlers, M. R., and Riordan, J. F. (1997) Identification of N-linked glycosylation sites in human testis angiotensin-converting enzyme and expression of an active deglycosylated form. *J. Biol. Chem. 272*, 3511–3519.
25. Balyasnikova, I. V., Metzger, R., Franke, F. E., and Danilov, S. M. (2003) Monoclonal antibodies to denatured human ACE (CD 143), broad species specificity, reactivity on paraffin sections, and detection of subtle conformational changes in the C-terminal domain of ACE. *Tissue Antigens 61*, 49–62.
26. Corradi, H. R., Schwager, S. L., Nchinda, A. T., Sturrock, E. D., and Acharya, K. R. (2006) Crystal structure of the N domain of human somatic angiotensin I-converting enzyme provides a structural basis for domain-specific inhibitor design. *J. Mol. Biol. 357*, 964–974.
27. Gordon, K., Redelinghuys, P., Schwager, S. L., Ehlers, M. R., Papageorgiou, A. C., Natesh, R., Acharya, K. R., and Sturrock, E. D. (2003) Deglycosylation, processing and crystallization of human testis angiotensin-converting enzyme. *Biochem. J. 371*, 437–442.
28. Ehlers, M. R., and Riordan, J. F. (1991) Angiotensin-converting enzyme: zinc- and inhibitor-binding stoichiometries of the somatic and testis isozymes. *Biochemistry 30*, 7118–7126.
29. Deddish, P. A., Wang, J., Michel, B., Morris, P. W., Davidson, N. O., Skidgel, R. A., and Erdös, E. G. (1994) Naturally occurring active N-domain of human angiotensin I-converting enzyme. *Proc. Natl. Acad. Sci. U.S.A. 91*, 7807–7811.
30. Friedland, J., and Silverstein, E. (1976) A sensitive fluorimetric assay for serum angiotensin-converting enzyme. *Am. J. Clin. Pathol. 66*, 416–424.
31. Schwager, S. L., Carmona, A. K., and Sturrock, E. D. (2006) A high-throughput fluorimetric assay for angiotensin I-converting enzyme. *Nat. Protoc. 1*, 1961–1964.
32. Araujo, M. C., Melo, R. L., Cesari, M. H., Juliano, M. A., Juliano, L., and Carmona, A. K. (2000) Peptidase specificity characterization of

C- and N-terminal catalytic sites of angiotensin I-converting enzyme. *Biochemistry 39*, 8519–8525.
33. Eisenthal, R., and Cornish-Bowden, A. (1974) The direct linear plot. A new graphical procedure for estimating enzyme kinetic parameters. *Biochem. J. 139*, 715–720.
34. Dixon, M. (1953) The determination of enzyme inhibitor constants. *Biochem. J. 55*, 170–171.
35. Jullien, N. D., Cuniasse, P., Georgiadis, D., Yiotakis, A., and Dive, V. (2006) Combined use of selective inhibitors and fluorogenic substrates to study the specificity of somatic wild-type angiotensin-converting enzyme. *FEBS J. 273*, 1772–1781.
36. Tzakos, A. G., and Gerothanassis, I. P. (2005) Domain-selective ligand-binding modes and atomic level pharmacophore refinement in angiotensin I converting enzyme (ACE) inhibitors. *ChemBioChem 6*, 1089–1103.
37. Cohen, G. H. (1997) ALIGN: a program to superimpose protein coordinates, accounting for insertions and deletions. *J. Appl. Crystallogr. 30*, 1160–1161.